POWERDRESS and HDA9 interact and promote histone H3 deacetylation at specific genomic sites in *Arabidopsis*

Yun Ju Kim[a,b,1,2], Ruozhong Wang[a,c,1], Lei Gao[d], Dongming Li[e], Chi Xu[d], Hyunggon Mang[b], Jien Jeon[b], Xiangsong Chen[f], Xuehua Zhong[f], June M. Kwak[b,g], Beixin Mo[d], Langtao Xiao[c], and Xuemei Chen[a,d,h,2]

[a]Department of Botany and Plant Sciences, Institute of Integrative Genome Biology, University of California, Riverside, CA 92521; [b]Center for Plant Aging Research, Institute for Basic Science, Daegu 305-811, South Korea; [c]College of Bioscience and Biotechnology, Hunan Agricultural University, Changsha 410128, China; [d]Guangdong Provincial Key Laboratory for Plant Epigenetics, College of Life Sciences and Oceanography, Shenzhen University, Shenzhen 518060, China; [e]School of Life Sciences, Lanzhou University, Lanzhou 730000, China; [f]Laboratory of Genetics, Wisconsin Institutes for Discovery, University of Wisconsin–Madison, Madison, WI 53706; [g]Department of New Biology, Daegu Gyeongbuk Institute of Science and Technology, Daegu 42988, Republic of Korea; and [h]Howard Hughes Medical Institute, University of California, Riverside, CA 92521

Contributed by Xuemei Chen, November 11, 2016 (sent for review September 29, 2016; reviewed by Wen-Hui Shen and Yanhai Yin)

Histone acetylation is a major epigenetic control mechanism that is tightly linked to the promotion of gene expression. Histone acetylation levels are balanced through the opposing activities of histone acetyltransferases (HATs) and histone deacetylases (HDACs). *Arabidopsis* HDAC genes (*AtHDACs*) compose a large gene family, and distinct phenotypes among *AtHDAC* mutants reflect the functional specificity of individual *AtHDACs*. However, the mechanisms underlying this functional diversity are largely unknown. Here, we show that POWERDRESS (PWR), a SANT (SWI3/DAD2/N-CoR/TFIII-B) domain protein, interacts with HDA9 and promotes histone H3 deacetylation, possibly by facilitating HDA9 function at target regions. The developmental phenotypes of *pwr* and *hda9* mutants were highly similar. Three lysine residues (K9, K14, and K27) of H3 retained hyperacetylation status in both *pwr* and *hda9* mutants. Genome-wide H3K9 and H3K14 acetylation profiling revealed elevated acetylation at largely overlapping sets of target genes in the two mutants. Highly similar gene-expression profiles in the two mutants correlated with the histone H3 acetylation status in the *pwr* and *hda9* mutants. In addition, *PWR* and *HDA9* modulated flowering time by repressing *AGAMOUS-LIKE 19* expression through histone H3 deacetylation in the same genetic pathway. Finally, PWR was shown to physically interact with HDA9, and its SANT2 domain, which is homologous to that of subunits in animal HDAC complexes, showed specific binding affinity to acetylated histone H3. We therefore propose that PWR acts as a subunit in a complex with HDA9 to result in lysine deacetylation of histone H3 at specific genomic targets.

SANT domain | POWERDRESS | HDA9 | histone deacetylation | AGL19

Posttranslational modifications of histones—including acetylation, methylation, phosphorylation, and ubiquitination—play important roles in plant development, genome integrity, and stress responses. Histone acetylation/deacetylation, a reversible process, promotes/represses gene expression (1) and occurs at lysine residues within histone N-terminal tails. The histone acetylation status is regulated by counteracting enzymes: histone acetyltransferases (HATs) and histone deacetylases (HDACs). The 18 HDACs identified in *Arabidopsis* (2) can be categorized into three groups based on phylogenetic analysis: reduced potassium dependency-3/histone deacetylase-1 (*RPD3*/*HDA1*), histone deacetylase-2 (*HD2*), and silent information regulator-2 (*SIR2*)-like (3). Twelve HDACs belong to the *RPD3*/*HDA1* group (3) and are involved in various biological processes, such as organ development, reproductive processes, hormone signaling, and DNA methylation (4–9). They can be further classified into three classes based on sequence homology (3). The *HD2* group is plant-specific and includes four HDACs that act in plant development and stress responses (10–13). The two HDACs encoded by the *SIR2* family genes in *Arabidopsis*, *SRT1* and *SRT2*, regulate mitochondrial energy metabolism and cellular dedifferentiation, respectively (14, 15).

In general, histone-modifying enzymes are components of multisubunit protein complexes, and interaction partners are thought to modulate enzymatic activity, substrate binding specificity, and cofactor recruitment. HDAC-interacting proteins in *Arabidopsis* include chromatin-modifying enzymes and transcription factors. The interaction partners responsible for specific biological functions of HDACs are best understood for *HDA6* and *HDA19* belonging to the *RPD3*/*HDA1*-class I genes (*HDA6*, *HDA7*, *HDA9*, and *HDA19*). *HDA6* controls flowering time, stress response, and gene silencing through its interacting partners (13, 16–20). HDA6 associates with histone demethylase and FLOWERING LOCUS D, as well as homologs of the human histone binding proteins RbAp46/48, FVE, and MSI5 to ensure proper flowering time (16, 18, 19, 21). In addition, HDA6 physically interacts with the DNA methyltransferase MET1 and regulates a subset of transposons and repeats (17). HDA6 and HDA19 also form complexes with various transcription factors (22–26). The corepressor TOPLESS complexes with HDA6 and PSEUDO RESPONSE REGULATORs to control circadian clock function (23). HDA19 participates in brassinosteroid signaling and basal defense through its interaction with the transcription factors BRASSINAZOLE RESISTANT1 (BZR1) and

Significance

Histone deacetylases (HDACs) belong to a large protein family in plants, and little is known about how target specificity of each HDAC is achieved. We show that a paired SANT (SWI3/DAD2/N-CoR/TFIII-B) domain-containing protein, POWERDRESS, specifically acts with HDA9 to confer the deacetylation of histone H3 lysine residues at a set of genomic targets to regulate various biological processes. Our study elucidates the functional correlation between SANT domain-containing proteins and HDACs in plants.

Author contributions: Y.J.K., J.M.K., B.M., L.X., and Xuemei Chen designed research; Y.J.K., R.W., D.L., C.X., H.M., J.J., and Xiangsong Chen performed research; Y.J.K., R.W., L.G., X.Z., and Xuemei Chen analyzed data; and Y.J.K. and Xuemei Chen wrote the paper.

Reviewers: W.-H.S., CNRS–Université de Strasbourg; and Y.Y., Iowa State University.

The authors declare no conflict of interest.

Freely available online through the PNAS open access option.

Data deposition: The data reported in this paper have been deposited in the Gene Expression Omnibus (GEO) database, www.ncbi.nlm.nih.gov/geo (accession no. GSE89770).

[1]Y.J.K. and R.W. contributed equally to this work.

[2]To whom correspondence may be addressed. Email: yjkim77@ibs.re.kr or xuemei.chen@ucr.edu.

This article contains supporting information online at www.pnas.org/lookup/suppl/doi:10.1073/pnas.1618618114/-/DCSupplemental.

WRKY 38/62, respectively (24, 26). The interacting partners of HDA9 have been elusive.

SANT (SWI3/DAD2/N-CoR/TFIII-B) domain-containing proteins exist as subunits of many chromatin remodeling complexes, such as histone acetylases, HDACs, and ATP-dependent chromatin-remodeling enzymes in yeast and animals (27, 28). The SANT domain was first described in nuclear receptor corepressors (N-CoR) and later found in the subunits of other chromatin-modifying complexes and transcription factors, including ADA, SWI-SNF, and TFIII-B (27). SANT domain function is tightly linked to enzymatic activity and substrate affinity. Deletion of the SANT domain in ADA2, a subunit of HATs, results in attenuated HAT activity and binding ability to unacetylated histone H3 tails (29, 30). Paired SANT domains (SANT1 and SANT2) are present in the corepressors SMRT (silencing mediator of retinoid and thyroid receptors), N-CoR (an HDAC3 complex subunit), and CoREST (an HDAC1 complex subunit) (27, 31). The two SANT domains have distinct roles in terms of HDAC function: SANT1 is responsible for HDAC activity and protein interaction, whereas SANT2 is necessary for substrate recognition (31–33). In contrast to the in-depth study of SANT domain-containing proteins in yeast and animals, the functions of SANT domain-containing proteins and their interaction partners in plants remain unclear.

POWERDRESS (*PWR*) encodes a protein with two SANT domains in *Arabidopsis* (34). A *pwr* mutant was isolated as an enhancer of *ag-10*, a weak allele of *AGAMOUS* (*AG*); the *pwr ag-10* double-mutant had prolonged floral stem cell activity, suggesting that *PWR* promotes the termination of floral stem cell fate. The *pwr* single-mutant exhibited other developmental defects, including bulged silique tips and early flowering. The broad spectrum of developmental defects of the *pwr* mutant indicates that *PWR* is involved in diverse biological processes. Although *PWR*'s role in floral stem cell regulation can be explained by its positive effects on the expression of a subset of *MIR172* genes and *CRABS CLAW* (*CRC*), how it affects other aspects of plant development is unknown. Furthermore, the molecular function of *PWR* in gene regulation is unknown.

Here, we show that PWR acts in association with HDA9 to repress gene expression through histone deacetylation. The SANT2 domain of PWR binds acetylated histone H3, including acetylated H3K9 and H3K14. The high degree of similarity between *pwr* and *hda9* mutants in terms of both morphological phenotypes and the hyperacetylation status of histone H3 suggests a functional link between *PWR* and *HDA9*. Indeed, PWR and HDA9 participate in histone H3K9 and H3K14 deacetylation and repression of gene expression at highly overlapping sets of genomic targets. One such target is *AGL19*, the misregulation of which was previously associated with the early-flowering phenotype of *hda9* mutants (35). We show that PWR and HDA9 act together on *AGL19* in the regulation of flowering time. Moreover, PWR and HDA9 were found to physically interact. Taken together, these findings suggest that a PWR–HDA9 complex regulates histone H3 deacetylation to control various biological processes.

Results

The PWR SANT2 Domain Preferentially Binds Modified Histone H3. We reported previously that *PWR* regulates floral stem cell fate through promotion of miR172 and *CRC* expression (34), but its molecular function was unknown. The paired SANT domains (SANT1 and SANT2), a distinct feature of PWR, were found to have high sequence similarity with the animal HDAC subunits SMRT and N-CoR (52% and 63% similarity, respectively) (Fig. S1). The SANT1 and SANT2 domains of SMRT are necessary for HDAC activity and binding to unmodified histone tails, respectively (32). To test whether the PWR SANT domains have similar functions to those of the SMRT SANT domains, a histone peptide array was probed with purified recombinant His-PWR SANT1, His-PWR SANT2, and His-PWR SANT1+SANT2 (Fig. S2). Although the PWR SANT1 domain did not bind any histone peptides (Fig. S2*B*), the SANT2 domain strongly bound to a subset of modified histone H3 but did not show any affinity for histone H4 or H2A/B; this binding preference was perfectly repeated in duplicated arrays in the same chip (Fig. 1*A* and Fig. S2*A*). The PWR SANT1+SANT2 also bound the same peptides (Fig. S2*C*). Because SANT1 did not bind histone peptides, the SANT1+SANT2 data independently verified the SANT2 binding specificities. Among monomodified H3, PWR SANT2 selectively bound to K9me1, K9me2, K9ac, S10P, T11P, and K14ac compared with unmodified H3 or H3K4ac. It also interacted with 32 kinds of multimodified histone H3, 29 of which contained at least one of the above modifications bound by His-PWR SANT2 (Fig. 1 and Table S1). Modifications at the H3K9 residue were the most preferred by the PWR SANT2 domain among the histone H3 monomodifications (~70%) (Fig. 1*B*). This finding suggests that the PWR SANT2 domain recognizes modified histone H3 and raises the possibility that *PWR* is functionally relevant in histone modifications.

***PWR* Specifically Promotes Histone H3 Deacetylation.** In light of the sequence similarity of the PWR SANT2 domain to that of HDAC subunits and its affinity for H3K9ac and H3K14ac, the effect of PWR on histone H3 acetylation status was analyzed. Histone H3 and H4 acetylation levels were examined by Western blotting using pan-acetylated H3 and H4 antibodies. Consistent with the histone peptide array results, hyperacetylation of histone H3 was observed in *pwr-2*, whereas no difference was observed for histone H4 acetylation (Fig. 2*A*). The levels of histone H3 acetylation at K9, K14, and K27 were all increased in *pwr-2*

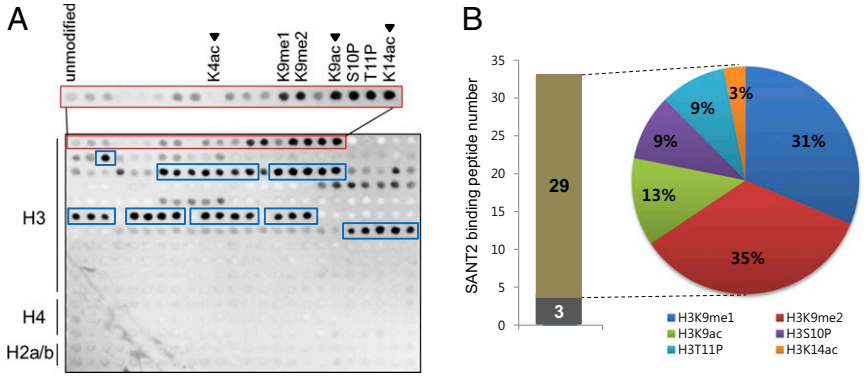

Fig. 1. The PWR SANT2 domain interacts with a subset of acetylated lysine residues of histone H3. (*A*) Histone peptide array analysis of the binding of the PWR SANT2 domain to histone peptides. Darker spots indicate stronger interaction between the PWR SANT2 domain and histone peptides. The red box includes unmodified and monomodified histone H3 peptides. PWR SANT2 binds strongly to six monomodified histone H3 peptides (K9me1, K9me2, K9ac, S10P, T11P, and K14ac). Note that, of the acetylated marks, PWR SANT2 binds K9ac and K14ac, but not K4ac (arrowheads). PWR SANT2-bound, multimodified histone H3 peptides are marked by blue boxes. (*B*) Graph and pie chart showing the representation of the six PWR SANT2-bound, monomodified histone H3 peptide species among 32 PWR SANT2-bound, multimodified histone H3 peptides. The gray and brown bars show the number of PWR SANT2-bound, multimodified histone H3 peptides that do not contain and contain PWR SANT2-bound monomodified histone H3 peptide species, respectively. The percentages in the pie chart indicate the occurrence rate of PWR SANT2-bound monomodified histone H3 peptide species.

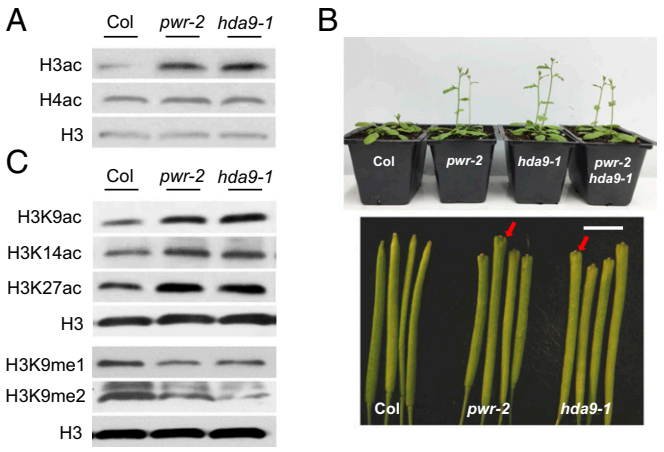

Fig. 2. PWR and HDA9 are specifically required for histone H3 deacetylation. (*A* and *C*) Western blot analysis of histone H3 acetylation levels. Total protein extract was resolved on an SDS/PAGE gel and blotted against pan-acetylated H3 (*A*) and acetylated-H3K9/H3K14/H3K27 and mono/dimethylated-H3K9antibodies (*C*). H3 was used as an internal control. (*B*) Phenotypes of *pwr-2*, *hda9-1*, and *pwr-2 hda9-1*. Plants were grown under continuous light. Note the enlarged silique tips in *pwr-2* and *hda9-1* (arrows). (Scale bar, 4 mm.)

(Fig. 2*C*). These results suggest that *PWR* may contribute to the regulation of histone H3 acetylation.

To investigate the functional correlation between PWR and HDACs, we screened several *hda* mutants for similarities with *pwr* mutants in morphology. From both the screen and published reports, the phenotype of *hda9* mutants was similar to that of *pwr* mutants, including early flowering and slightly bulged silique tips (Fig. 2*B* and Fig. S3) (35, 36). The early flowering phenotype was much milder under continuous light compared with short-day conditions (35, 36), such that *pwr-2* and *hda9-1* mutants bolted about 1.5 d earlier than wild type, with a similar number of rosette leaves to that in wild type at bolting (Fig. S3). Additionally, the acetylation levels of histone pan-H3, but not pan-H4, were increased in the *hda9* mutant (Fig. 2*A*). H3K9 and H3K14 acetylation levels were also increased in *hda9* (Fig. 2*C*). Hyperacetylation of H3K27 in the *hda9* mutant was reported in a previous study (35) and was also observed here (Fig. 2*C*). The similar morphological and histone acetylation phenotypes of the two mutants led us to hypothesize that *PWR* and *HDA9* act closely to deacetylate histone H3 at specific target genes.

PWR and HDA9 Enhance Histone H3 Deacetylation at Largely Overlapping Sets of Targets. To determine whether PWR promotes deacetylation at specific genomic targets and, if so, whether PWR and HDA9 affect the same targets, a global analysis of the acetylation status of histone H3K9 and H3K14 was conducted. Chromatin immunoprecipitation (ChIP) high-throughput sequencing (ChIP-seq) was performed in wild type, *pwr-2*, and *hda9-1* using antibodies against H3K9ac and H3K14ac. For H3K9ac ChIP-seq, two biological replicates were performed; Pearson's correlation analysis showed that the replicates were reasonably reproducible (Fig. S4). H3K14ac ChIP-seq was carried out with one replicate, but randomly selected observations were later validated by ChIP-quantitative PCR (ChIP-qPCR) (Fig. S5). In wild type, a total of 12,650 H3K9ac peaks were found. As observed before (37, 38), the peaks were mostly in genes or intergenic regions (Fig. S6*A*). For the H3K14ac ChIP-seq, a total of 11,141 H3K14ac peaks were found. The genomic distribution of H3K14ac was similar to that of H3K9ac, but a stronger enrichment for genic regions than H3K9ac was found (Fig. S6*B*). Within genes, H3K9ac and H3K14ac marks were strongly enriched in 5′UTRs, which constitute 4% of all genes (Fig. S6*E*) but more than 25% of H3K9ac- or H3K14ac-containing genic regions (Fig. S6 *C* and *D*). In addition, H3K9 and H3K14 acetylation was centered at ∼300 bp downstream of the transcriptional start site (TSS) and markedly dropped off at the transcription termination site (TTS) (Fig. 3*D*).

Next, we identified differentially acetylated regions between each mutant and wild type. Among the differentially acetylated regions identified, the majority were hyperacetylated in *pwr-2* (H3K9ac: 3,921 of 5,026; H3K14ac: 3,128 of 3,351) and *hda9-1* (H3K9ac: 4,222 of 5,307; H3K14ac: 3,847 of 4,131) compared with wild type (Col) (Fig. 3*A*), which is consistent with the

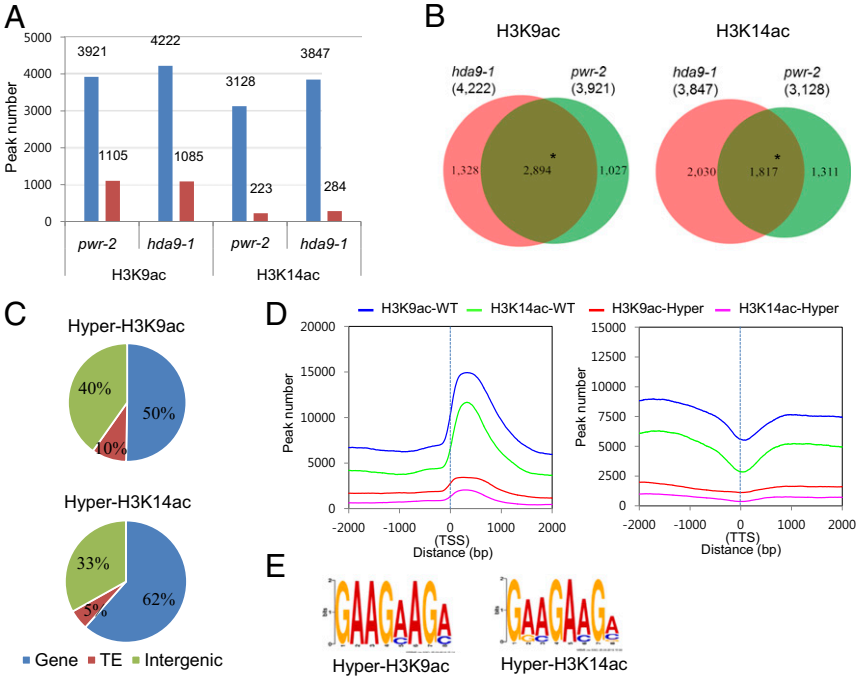

Fig. 3. Hyperacetylated H3K9 and H3K14 regions in *pwr* and *hda9* significantly overlap. (*A*) Histogram showing ChIP-seq–derived differentially acetylated regions for H3K9 and H3K14 in *pwr-2* and *hda9-1*. Blue and red bars represent hyper- and hypoacetylation, respectively. (*B*) Venn diagram showing the overlap of hyperacetylation ChIP peaks between *pwr-2* and *hda9-1*. *$P = 0$ (hypergeometric test). (*C*) Pie charts showing the genomic distribution of overlapping hyperacetylation ChIP peaks in *pwr-2* and *hda9-1* from *B*. (*D*) The distribution of all ChIP peaks in wild type (blue and green curves) and overlapping hyperacetylation ChIP peaks in *pwr-2* and *hda9-1* (red and magenta curves) around the TSS (*Left*) and TTS (*Right*) of protein-coding genes. (*E*) The motifs significantly enriched in hyperacetylation ChIP peaks in *pwr-2* and *hda9-1* through MEME-ChIP analysis.

observed increase in H3K9ac and H3K14ac levels in the two mutants (Fig. 2*C*). The hyperacetylated regions accounted for 30–40% of all ChIP-derived peaks for H3K9 (*pwr-2*: 3,921 of 12,890; *hda9-1*: 4,222 of 12,745) and H3K14 (*pwr-2*: 3,128 of 12,791; *hda9-1*: 3,847 of 13,122) in the *pwr* and *hda9* mutants, which reflects that PWR and HDA9 contribute to more than one-third of H3K9 and H3K14 deacetylation at a genome-wide level. Comparative analysis of the hyperacetylated regions in *pwr-2* and *hda9-1* revealed significant overlap: about 70% overlap for H3K9ac ($P = 0$; hypergeometric test) and 50–60% overlap for H3K14ac ($P = 0$; hypergeometric test) (Fig. 3*B*). Further analysis of the overlapping regions of hyperacetylated H3K9 and H3K14 between *pwr-2* and *hda9-1* revealed that more than 50% corresponded to genes and a minor fraction corresponded to transposable elements (TEs) (Fig. 3*C*), which is consistent with the nature of H3K9ac and H3K14ac as euchromatic marks. Furthermore, in the overlapping, hyperacetylated regions, H3K9 and H3K14 acetylation was peaking at ∼300 bp downstream of the TSS, as observed in wild type (Fig. 3*D*). MEME-ChIP analysis (39) was performed to identify overrepresented motifs among the genomic targets of *PWR* and *HDA9* in terms of histone H3K9 and H3K14 deacetylation. Similarly, motifs GAAG(A/C)AG(A/C) and G(A/G)(A/C)GA(A/C)G(A/C/G) were identified as the most significant motifs for H3K9ac and H3K14ac marks, respectively, from overlapping hyperacetylation regions between *pwr-2* and *hda9-1* (Fig. 3*E*). These findings indicate that *PWR* and *HDA9* regulate histone H3 deacetylation mainly at actively transcribed regions and that the functions of these two genes are tightly correlated.

***PWR* and *HDA9* Share a Significant Number of Target Genes.** The studies above revealed hyperacetylation at common genomic sites in the *pwr* and *hda9* mutants, raising the possibility that the two genes regulate similar sets of target genes. Transcriptome analysis was performed to examine the correlation between the histone acetylation status and gene-expression levels of the targets of *PWR* and *HDA9*. In *pwr-2* and *hda9-1*, 2,159 and 2,073 differentially expressed genes (DEGs) were identified, respectively (Fig. 4*A*). Among the DEGs, 774 and 1,385 genes were increased and reduced in *pwr-2*, respectively, and 772 and 1,301 genes were increased and reduced in *hda9*-1, respectively (Fig. 4*A*). There was a significant overlap between the DEGs identified in *pwr-2* and *hda9*-1 [542 increased DEGs and 817 reduced DEGs, $P = 0$ (hypergeometric test)] (Fig. 4*A*), indicating that PWR and HDA9 act in the same regulatory pathway. Gene ontology (GO) analysis revealed that the up-regulated genes in *pwr-2* and *hda9-1* were mainly involved in stress responses (Fig. 4*D*). Further analysis was performed to assess the correlation between overlapping up-regulated DEGs and ChIP-derived hyperacetylated regions in the corresponding gene body and promoter regions (up to 2-kb upstream of the TSSs). Of the 542 genes identified as up-regulated DEGs in both mutants (i.e., co–up-regulated DEGs), 179 and 144 genes were hyperacetylated at H3K9 and H3K14, respectively, in the gene body or promoter regions in *pwr-2* or *hda9-1* (Fig. 4*B*). About 50% of the hyperacetylated DEGs for H3K9 and H3K14 overlapped between *pwr-2* and *hda9-1* (H3K9: 89 of 137 in *pwr-2* and 89 of 131 in *hda9-1*; H3K14: 47 of 86 in *pwr-2* and 47 of 105 in *hda9-1*) (Fig. 4*B*). Furthermore, 274 of the 542 co–up-regulated DEGs retained hyperacetylation status for either H3K9 or H3K14 (Fig. 4*C*). About 30% (49 of 179 for H3K9 and 49 of 144 for H3K14) had both H3K9 and H3K14 hyperacetylation (Fig. 4*C*), suggesting some degree of functional specificity between H3K9 and H3K14 acetylation of target genes. Taken together, these findings indicate that histone deacetylation at either H3K9 or H3K14 through PWR and HDA9 is significantly correlated with gene expression at the target loci.

***PWR* and *HDA9* Act in the Same Genetic Pathway Through *AGL19* to Ensure Proper Flowering Time.** One of the obvious phenotypes of *pwr* and *hda9* mutants is early flowering (Fig. 2*B*). Several studies have shown that early flowering in *hda9* is because of increased *AGL19* levels, which results from increased levels of histone acetylation and Pol II occupancy at the locus (35, 36). To investigate whether *PWR* acts in the *AGL19*-mediated flowering-time pathway through *HDA9* function, we first examined *AGL19* transcript levels in *pwr-2*. *AGL19* expression was higher in *pwr-2* as in *hda9-1* (Fig. 5*A*). Next, the acetylation level of histone H3 was tested in *pwr-2* and *hda9-1* by ChIP-qPCR, and the analysis revealed increased histone H3 acetylation in *pwr-2* and *hda9-1* (Fig. 5*B*). Finally, no synergetic effect was observed in the *pwr-2 hda9-1* double-mutant compared with either single-mutant in terms of *AGL19* transcript levels and flowering time (Figs. 2*B*

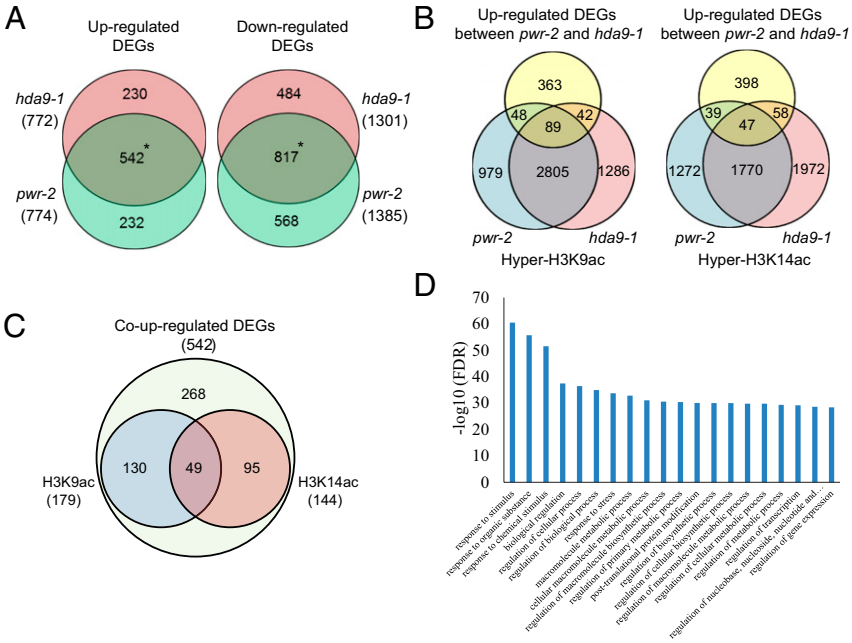

Fig. 4. Histone deacetylation through *PWR* and *HDA9* correlates with gene expression. (*A*) Venn diagrams showing the overlapping up-regulated (*Left*) and down-regulated (*Right*) DEGs identified in *pwr-2* and *hda9-1* (i.e., coregulated DEGs). *$P = 0$ (hypergeometric test). (*B*) Venn diagrams showing the overlap of co–up-regulated DEGs and hyperacetylated H3K9 (*Left*) or hyperacetylated H3K14 (*Right*) in *pwr-2* and *hda9-1*. (*C*) Venn diagram showing the status of H3K9 or H3K14 hyperacetylation in either *pwr-2* or *hda9-1* among the 542 co–up-regulated DEGs. (*D*) GO term analysis of co–up-regulated DEGs in *pwr-2* and *hda9-1*. FDR, false-discovery rate.

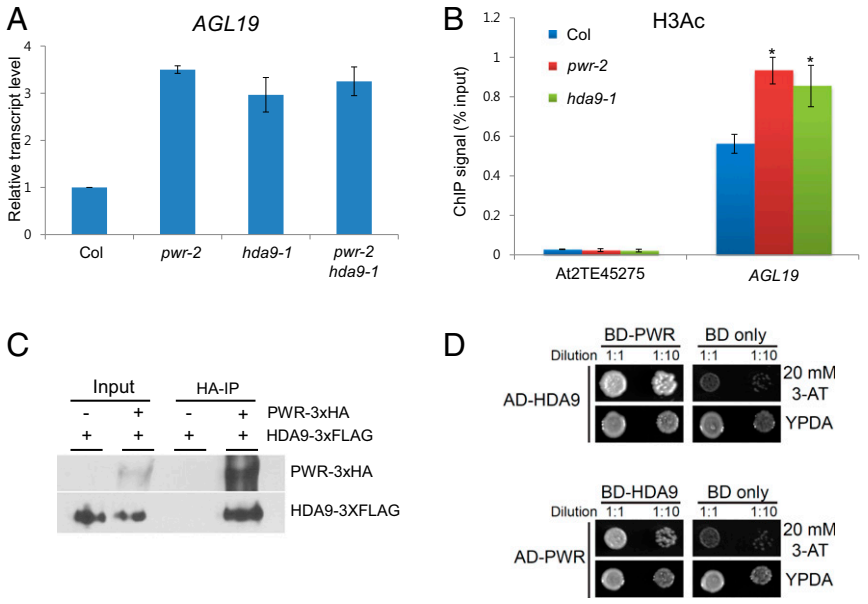

Fig. 5. The PWR–HDA9 complex regulates flowering time through *AGL19*. (*A*) Quantitative RT-PCR analysis of *AGL19* expression in *pwr-2*, *hda9-1*, and *pwr-2 hda9-1*. *AGL19* transcript levels were normalized to *UBQ5* and compared with Col (wild type). (*B*) The acetylation status of histone H3 at the *AGL19* locus in *pwr-2* and *hda9-1* determined by ChIP. AT2TE45275 was used as a negative control. Error bars indicate SD derived from two biological replicates. $*P < 0.05$. (*C*) Coimmunoprecipitation (co-IP) experiment showing the interaction between PWR-3xHA and HDA9-3XFLAG in a tobacco transient-expression assay. (*D*) Yeast two-hybrid confirmation of PWR–HDA9 interaction. The interaction was tested with SD-Leu/-Trp/-His media with 20 mM 3-amino-1,2,4-triazole (3-AT). Yeast grown on normal media (YPDA) served as a control. AD, activation domain; BD, binding domain.

and 5*A* and Fig. S3). Taken together, these findings indicate that *PWR* and *HDA9* act in the same genetic pathway in the regulation of flowering time.

PWR Physically Interacts with HDA9. Our results indicate that the functions of *PWR* and *HDA9* are tightly correlated: they share histone deacetylation targets and regulate some of the same biological processes. Because N-CoR/SMRT acts together with HDAC3 as a subunit of the complex (32), we investigated whether PWR is associated with HDA9. HA epitope-fused PWR (PWR-3xHA) and FLAG epitope-tagged HDA9 (HDA9-3xFLAG) were transiently expressed in *Nicotiana benthamiana*. Immunoprecipitation was performed with anti-HA antibodies to pull down PWR-3xHA followed by Western blotting to detect HDA9-3xFLAG. Indeed, HDA9-FLAG was enriched in the PWR-3xHA immunoprecipitate (Fig. 5*C*). To confirm the interaction between PWR and HDA9, we performed a yeast two-hybrid assay and PWR was found to interact with HDA9 (Fig. 5*D*). These results suggest that PWR interacts with HDA9 and may function in the same complex.

Discussion

The presence of a pair of SANT domains in PWR and their high sequence similarity to those of animal HDAC subunits were a major clue in the investigation of the molecular function of PWR. We found that the PWR SANT2 domain recognizes histones, as does the SANT2 motif of the HDAC-associated subunit SMRT/N-CoR. This finding prompted further studies on *PWR* and HDACs and led to the conclusion that PWR acts together with HDA9 to deacetylate H3K9 and H3K14 at numerous genes. Unlike the specific binding of the SMRT SANT2 domain to an unacetylated histone H4 tail (32), the PWR SANT2 domain preferentially binds to acetylated histone H3. Yu et al. (32) proposed that the SMRT SANT2 domain binds to unacetylated histone H4, possibly to recruit other cofactors or to prohibit further modification. In contrast, the binding of the PWR SANT2 domain to targets probably promotes histone H3 deacetylation in plants. The PWR SANT2 domain exhibited specificity for modified histone H3 but not H4 or H2A/B (Fig. 1*A*), which is consistent with the hyperacetylation status in *pwr-2* and *hda9-1* being specific for histone H3 and not H4 (35 and present study). Given the interaction between PWR and HDA9 and the significant overlap in their deacetylation targets in the genome, we propose that the PWR SANT2 domain confers substrate binding preferences to HDA9.

HDA9 regulates several biological processes, such as flowering time, seed dormancy, and stress responses (14, 35, 36, 40, 41). Although previous studies have shown that development and stress-response genes are up-regulated and this is accompanied by hyperacetylation in the *hda9* mutant, there have been no reports about HDA9-interacting proteins required for its histone deacetylation function. The physical interaction between HDA9 and PWR and the similar morphological and molecular defects in the *pwr* and *hda9* mutants support the hypothesis that PWR and HDA9 act in the same complex. However, it is not clear whether HDA9 is the only interacting partner of PWR. The histone peptide array showed that in addition to acetylated histone H3, the PWR SANT2 domain also bound to other modified histone H3, such as H3K9me1 and H3K9me2 (Fig. 1*A*), and the levels of H3K9me1 and H3K9me2 were reduced in *pwr-2* and *hda9-1* (Fig. 2*C*). This finding raises two possibilities. First, the PWR–HDA9 complex coordinates histone acetylation and methylation for transcriptional regulation. For example, PWR may act as a histone code reader of which the SANT2 domain recognizes H3K9me1/me2 and interprets its repressive mode through histone deacetylation by recruiting HDA9. Because H3K9me1/me2 is mainly found at heterochromatin, this may be a mechanism to prevent histone acetylation at such genomic regions. Second, PWR acts in a distinct complex from the one containing HDA9 to regulate other histone modifications. Several histone demethylases are known to interact with N-CoR. For example, JMJD2A, which demethylases di- or trimethylated histone H3K9, was isolated from affinity purification of the N-CoR complex (42).

Our previous study revealed that *PWR* regulates floral stem cells as a positive regulator of a subset of *MIR172* genes and *CRC* (34). Given our finding that PWR acts in histone H3 deacetylation, the reduced transcript levels of *MIR172* and *CRC* in *pwr* may be an indirect effect. In fact, there were a large number of down-regulated DEGs observed in *pwr-2* and *hda9-1* along with significant overlap between them (Fig. 4*A*). As an example, the level of miR164 was increased in *pwr-2* (34) and, consistently, ChIP-seq revealed H3K9 hyperacetylation at *MIR164b* in both *pwr-2* and *hda9-1*. Therefore, *MIR164b* could be a direct target of the PWR–HDA9 complex and increased miR164 levels are expected to result in reduced expression of miR164 target genes in *pwr* and *hda9* mutants. It is not yet clear

how the PWR–HDA9 complex specifies its targets. Motif analysis uncovered significant enrichment of sequences from the H3K9ac and H3K14ac ChIP-seq peaks (Fig. 3*E*), which are very similar to the GAAGAA motif. No transcription factors targeting this motif are known, but several studies have proposed that this motif is significantly enriched in splicing junction proximal exons, possibly as an exonic splicing enhancer (43–45). Therefore, the GAAGAA motif present in some genes may be recognized by PWR–HDA9 to regulate their transcription. Alternatively, the GAAGAA motif may simply be associated with histone acetylation in spliced genes, leading to an overrepresentation of this motif in the dataset rather than being directly targeted by the PWR–HDA9 complex.

Materials and Methods

For plant materials, histone peptide array, Western blot analysis, mRNA-seq, ChIP-seq, and other methods, please see *SI Materials and Methods*. See Table S2 for a list of the primers used. A summary of the ChIP-seq reads is provided in Table S3.

ACKNOWLEDGMENTS. We thank Dr. Jeongsik Kim for the plasmid gCsVMV-3xHA-N-1300; Dr. Hui Kyung Cho for technical support; and Rae Eden Yumul for editing the manuscript. This work was supported by NIH Grant GM061146 (to Xuemei Chen); Gordon and Betty Moore Foundation Grant GBMF3046 (to Xuemei Chen); Guangdong Innovation Research Team Fund 2014ZT05S078 (to Xuemei Chen); IBS-R013-G2 (to J.M.K. and Y.-J.K.); and National Natural Science Foundation of China Grants 31570372 and 31671777 (to R.W. and L.X.). Work in X.Z.'s laboratory was supported by National Science Foundation CAREER Award MCB-1552455, the Alexander von Humboldt Foundation (Alfred Toepfer Faculty Fellow Award), and US Department of Agriculture and National Institute of Food and Agriculture Grant Hatch 1002874.

1. Struhl K (1998) Histone acetylation and transcriptional regulatory mechanisms. *Genes Dev* 12(5):599–606.
2. Pandey R, et al. (2002) Analysis of histone acetyltransferase and histone deacetylase families of *Arabidopsis thaliana* suggests functional diversification of chromatin modification among multicellular eukaryotes. *Nucleic Acids Res* 30(23):5036–5055.
3. Hollender C, Liu Z (2008) Histone deacetylase genes in *Arabidopsis* development. *J Integr Plant Biol* 50(7):875–885.
4. Liu C, et al. (2013) HDA18 affects cell fate in *Arabidopsis* root epidermis via histone acetylation at four kinase genes. *Plant Cell* 25(1):257–269.
5. Cigliano RA, et al. (2013) Histone deacetylase AtHDA7 is required for female gametophyte and embryo development in *Arabidopsis*. *Plant Physiol* 163(1):431–440.
6. Zhou C, Zhang L, Duan J, Miki B, Wu K (2005) HISTONE DEACETYLASE19 is involved in jasmonic acid and ethylene signaling of pathogen response in *Arabidopsis*. *Plant Cell* 17(4):1196–1204.
7. Long JA, Ohno C, Smith ZR, Meyerowitz EM (2006) TOPLESS regulates apical embryonic fate in *Arabidopsis*. *Science* 312(5779):1520–1523.
8. Aufsatz W, Mette MF, van der Winden J, Matzke M, Matzke AJM (2002) HDA6, a putative histone deacetylase needed to enhance DNA methylation induced by double-stranded RNA. *EMBO J* 21(24):6832–6841.
9. Ryu H, Cho H, Bae W, Hwang I (2014) Control of early seedling development by BES1/TPL/HDA19-mediated epigenetic regulation of ABI3. *Nat Commun* 5:4138.
10. Wu K, Tian L, Malik K, Brown D, Miki B (2000) Functional analysis of HD2 histone deacetylase homologues in *Arabidopsis thaliana*. *Plant J* 22(1):19–27.
11. Zhou C, et al. (2004) Expression and function of HD2-type histone deacetylases in *Arabidopsis* development. *Plant J* 38(5):715–724.
12. Sridha S, Wu K (2006) Identification of AtHD2C as a novel regulator of abscisic acid responses in *Arabidopsis*. *Plant J* 46(1):124–133.
13. Luo M, et al. (2012) HD2C interacts with HDA6 and is involved in ABA and salt stress response in *Arabidopsis*. *J Exp Bot* 63(8):3297–3306.
14. Lee K, Park OS, Jung SJ, Seo PJ (2016) Histone deacetylation-mediated cellular dedifferentiation in *Arabidopsis*. *J Plant Physiol* 191:95–100.
15. König AC, et al. (2014) The *Arabidopsis* class II sirtuin is a lysine deacetylase and interacts with mitochondrial energy metabolism. *Plant Physiol* 164(3):1401–1414.
16. Yu CW, et al. (2011) HISTONE DEACETYLASE6 interacts with FLOWERING LOCUS D and regulates flowering in *Arabidopsis*. *Plant Physiol* 156(1):173–184.
17. Liu X, et al. (2012) HDA6 directly interacts with DNA methyltransferase MET1 and maintains transposable element silencing in *Arabidopsis*. *Plant Physiol* 158(1):119–129.
18. Gu X, et al. (2011) *Arabidopsis* homologs of retinoblastoma-associated protein 46/48 associate with a histone deacetylase to act redundantly in chromatin silencing. *PLoS Genet* 7(11):e1002366.
19. He Y, Michaels SD, Amasino RM (2003) Regulation of flowering time by histone acetylation in *Arabidopsis*. *Science* 302(5651):1751–1754.
20. Liu X, et al. (2013) PHYTOCHROME INTERACTING FACTOR3 associates with the histone deacetylase HDA15 in repression of chlorophyll biosynthesis and photosynthesis in etiolated *Arabidopsis* seedlings. *Plant Cell* 25(4):1258–1273.
21. Yu CW, Chang KY, Wu K (2016) Genome-wide analysis of gene regulatory networks of the FVE-HDA6-FLD complex in *Arabidopsis*. *Front Plant Sci* 7:555.
22. Zhou Y, et al. (2013) HISTONE DEACETYLASE19 interacts with HSL1 and participates in the repression of seed maturation genes in *Arabidopsis* seedlings. *Plant Cell* 25(1):134–148.
23. Wang L, Kim J, Somers DE (2013) Transcriptional corepressor TOPLESS complexes with pseudoresponse regulator proteins and histone deacetylases to regulate circadian transcription. *Proc Natl Acad Sci USA* 110(2):761–766.
24. Wang C, et al. (2013) Identification of BZR1-interacting proteins as potential components of the brassinosteroid signaling pathway in *Arabidopsis* through tandem affinity purification. *Mol Cell Proteomics* 12(12):3653–3665.
25. Krogan NT, Hogan K, Long JA (2012) APETALA2 negatively regulates multiple floral organ identity genes in *Arabidopsis* by recruiting the co-repressor TOPLESS and the histone deacetylase HDA19. *Development* 139(22):4180–4190.
26. Kim KC, Lai Z, Fan B, Chen Z (2008) *Arabidopsis* WRKY38 and WRKY62 transcription factors interact with histone deacetylase 19 in basal defense. *Plant Cell* 20(9):2357–2371.
27. Aasland R, Stewart AF, Gibson T (1996) The SANT domain: A putative DNA-binding domain in the SWI-SNF and ADA complexes, the transcriptional co-repressor N-CoR and TFIIIB. *Trends Biochem Sci* 21(3):87–88.
28. Boyer LA, Latek RR, Peterson CL (2004) The SANT domain: A unique histone-tail-binding module? *Nat Rev Mol Cell Biol* 5(2):158–163.
29. Boyer LA, et al. (2002) Essential role for the SANT domain in the functioning of multiple chromatin remodeling enzymes. *Mol Cell* 10(4):935–942.
30. Sterner DE, Wang X, Bloom MH, Simon GM, Berger SL (2002) The SANT domain of Ada2 is required for normal acetylation of histones by the yeast SAGA complex. *J Biol Chem* 277(10):8178–8186.
31. You A, Tong JK, Grozinger CM, Schreiber SL (2001) CoREST is an integral component of the CoREST-human histone deacetylase complex. *Proc Natl Acad Sci USA* 98(4):1454–1458.
32. Yu J, Li Y, Ishizuka T, Guenther MG, Lazar MA (2003) A SANT motif in the SMRT corepressor interprets the histone code and promotes histone deacetylation. *EMBO J* 22(13):3403–3410.
33. Guenther MG, Barak O, Lazar MA (2001) The SMRT and N-CoR corepressors are activating cofactors for histone deacetylase 3. *Mol Cell Biol* 21(18):6091–6101.
34. Yumul RE, et al. (2013) POWERDRESS and diversified expression of the MIR172 gene family bolster the floral stem cell network. *PLoS Genet* 9(1):e1003218.
35. Kim W, Latrasse D, Servet C, Zhou DX (2013) *Arabidopsis* histone deacetylase HDA9 regulates flowering time through repression of AGL19. *Biochem Biophys Res Commun* 432(2):394–398.
36. Kang MJ, Jin HS, Noh YS, Noh B (2015) Repression of flowering under a noninductive photoperiod by the HDA9-AGL19-FT module in *Arabidopsis*. *New Phytol* 206(1):281–294.
37. Zhou J, et al. (2010) Genome-wide profiling of histone H3 lysine 9 acetylation and dimethylation in *Arabidopsis* reveals correlation between multiple histone marks and gene expression. *Plant Mol Biol* 72(6):585–595.
38. Sequeira-Mendes J, et al. (2014) The functional topography of the *Arabidopsis* genome is organized in a reduced number of linear motifs of chromatin states. *Plant Cell* 26(6):2351–2366.
39. Machanick P, Bailey TL (2011) MEME-ChIP: Motif analysis of large DNA datasets. *Bioinformatics* 27(12):1696–1697.
40. Zheng Y, et al. (2016) Histone deacetylase HDA9 negatively regulates salt and drought stress responsiveness in *Arabidopsis*. *J Exp Bot* 67(6):1703–1713.
41. van Zanten M, et al. (2014) HISTONE DEACETYLASE 9 represses seedling traits in *Arabidopsis thaliana* dry seeds. *Plant J* 80(3):475–488.
42. Zhang D, Yoon HG, Wong J (2005) JMJD2A is a novel N-CoR-interacting protein and is involved in repression of the human transcription factor achaete scute-like homologue 2 (ASCL2/Hash2). *Mol Cell Biol* 25(15):6404–6414.
43. Fairbrother WG, Yeh RF, Sharp PA, Burge CB (2002) Predictive identification of exonic splicing enhancers in human genes. *Science* 297(5583):1007–1013.
44. Ramchatesingh J, Zahler AM, Neugebauer KM, Roth MB, Cooper TA (1995) A subset of SR proteins activates splicing of the cardiac troponin T alternative exon by direct interactions with an exonic enhancer. *Mol Cell Biol* 15(9):4898–4907.
45. Sanford JR, et al. (2009) Splicing factor SFRS1 recognizes a functionally diverse landscape of RNA transcripts. *Genome Res* 19(3):381–394.
46. Kim D, Langmead B, Salzberg SL (2015) HISAT: A fast spliced aligner with low memory requirements. *Nat Methods* 12(4):357–360.
47. Robinson MD, McCarthy DJ, Smyth GK (2010) edgeR: A Bioconductor package for differential expression analysis of digital gene expression data. *Bioinformatics* 26(1):139–140.
48. Li C, et al. (2016) Concerted genomic targeting of H3K27 demethylase REF6 and chromatin-remodeling ATPase BRM in Arabidopsis. *Nat Genet* 48(6):687–693.
49. Langmead B, Trapnell C, Pop M, Salzberg SL (2009) Ultrafast and memory-efficient alignment of short DNA sequences to the human genome. *Genome Biol* 10(3):R25.
50. Robinson JT, et al. (2011) Integrative genomics viewer. *Nat Biotechnol* 29(1):24–26.
51. Zang C, et al. (2009) A clustering approach for identification of enriched domains from histone modification ChIP-Seq data. *Bioinformatics* 25(15):1952–1958.
52. Du Z, Zhou X, Ling Y, Zhang Z, Su Z (2010) agriGO: A GO analysis toolkit for the agricultural community. *Nucleic Acids Res* 38(Web Server issue):W64–W70.